Spin polarization of an electron-hole gas in InAs/GaSb quantum wells under a dc current

A. Zakharova,[1] I. Lapushkin,[1] K. Nilsson,[2] S. T. Yen,[3] and K. A. Chao[2]
[1]*Institute of Physics and Technology of the Russian Academy of Sciences, Nakhimovskii Avenue 34, Moscow 117218, Russia*
[2]*Department of Physics, Lund University, Sölvegatan 14A S-22362 Lund, Sweden*
[3]*Department of Electronics Engineering, National Chiao Tung University, Hsinchu, Taiwan, Republic of China*
(Received 16 November 2005; revised manuscript received 19 January 2006; published 24 March 2006)

We have investigated the spin polarization of electrons and holes in InAs/GaSb broken-gap quantum wells under nonequilibrium conditions when a dc electric field is applied parallel to interfaces. The existence of a nonzero asymmetric part of the quasiparticle distribution function caused by the dc current and the spin-split of the electron-hole hybridized states generates a finite spin polarization in both the InAs layer and the GaSb layer. With a very weak asymmetry of the distribution function, our self-consistent calculation yields about 1% spin polarization for electrons in the InAs layer and holes in the GaSb layer. The signs of these spin polarizations depend on the widths of the layers, changing the widths drives a phase transition in the electron-hole gas between the hybridized semiconducting phase and the normal semiconducting phase. In the hybridized semiconducting phase, the spin polarizations in both the InAs layer and the GaSb layer have the same sign. Crossing the phase boundary, the electron spin polarization and the total spin polarization in the InAs/GaSb quantum well can change their signs.

DOI: 10.1103/PhysRevB.73.125337 PACS number(s): 73.21.Ac, 73.21.Fg, 73.40.Kp

I. INTRODUCTION

Spin polarization of charge carriers in semiconductors, electrons, and/or holes, as well as the corresponding spin-polarized current have been much studied recently[1] for their importance in both fundamental research and spintronic applications. One focused area is the various mechanisms of spin polarization in different types of systems: quantum wells with a dc current or under a magnetic field,[2–10] and tunneling heterostructures with a current perpendicular to interfaces.[11–19] Two important effects, which can result in spin polarization, are the spin-split of energy levels in quantum wells and the spin-dependent tunneling probability in tunneling heterostructures. For nonmagnetic systems in the absence of an applied magnetic field, both effects have their origin in the spin-orbit interaction and the sample structural asymmetry, or the bulk inversion asymmetry. In almost all works on the spin polarization in nonmagnetic quantum wells, either the electron subsystem or the hole subsystem have been investigated separately.[2–7,9,10] In this work we will present a theory of spin polarization in a hybridized electron-hole gas in the absence of an applied magnetic field.

A hybridized electron-hole gas exists in broken-gap InAs/GaSb quantum wells sandwiched by wide-gap AlSb barriers. The InAs conduction band overlaps with the GaSb valence band. The amount of overlap depends on the lattice mismatch induced strain which can be varied by adjusting the layer thickness. Without strain this overlap is about 0.15 eV. Therefore, if the InAs layer is sufficiently thick at zero in-plane wave vector $k_{\parallel}=0$ the lowest electron level, in the InAs/GaSb quantum well, lies below the highest hole level. With increasing $k_{\parallel}$ the electronlike levels move upwards and the holelike levels move downwards, resulting in an anticrossing of subbands and formation of a hybridization gap in the in-plane dispersion. The system is then in the hybridized semiconducting phase which was analyzed theoretically[20–28] and observed experimentally.[22,29–32] In the hybridized semiconducting phase, electrons in InAs coexist with holes in GaSb if the Fermi level is between the lowest electron and the highest hole levels at $k_{\parallel}=0$. This phase changes to the normal semiconducting phase with a semiconducting gap when the InAs or the GaSb layer width is reduced, because the hole energy levels become lower than all electron levels. Such a complicated evolution of subband dispersions will certainly produce interesting phenomena in connection with spin polarization in the electron-hole gas.

Without an external magnetic field, the structure asymmetry of AlSb/InAs/GaSb/AlSb quantum wells and the spin-orbit interaction cause the spin split of subbands[8,23,25,27,28] due to the Rashba effect[33]. In strongly asymmetric structures, for sufficiently small in-plane wave vectors, this spin split of the two-dimensional (2D) carriers is much larger than that caused by the bulk inversion asymmetry.[8,34,35] Such spin split of levels in InAs/GaSb quantum wells caused by the Rashba effect was observed experimentally.[36] Analyzing the Shubnikov-de Haas oscillations, the authors of Ref. 36 deduced a spin split of 3.5 meV in the absence of a magnetic field for the ground electron level in a quantum well with a 7.5 nm InAs layer. The spin split of levels and the strain induced by the lattice mismatch, which significantly affects the carrier energy level structures,[27] will then play an important role in the spin polarization of the system. This is the main theme of the present work, which will be accomplished with calculations of energy levels and wave functions self-consistently with the potential distribution and Fermi level position in order to derive accurate results.

To study the spin polarization in AlSb/InAs/GaSb/AlSb quantum wells, we will use the eight-band $\mathbf{k}\cdot\mathbf{p}$ model with a dc current parallel to the interfaces. This dc current will generate a weak asymmetry in the carrier distribution function, and hence a nonzero spin polarization. We will show that the sign of the electron spin polarization in the InAs layer and the total spin polarization in the InAs/GaSb quantum well can change sign across the transition from the hybridized

 ©2006 The American Physical Society

semiconducting phase to the normal semiconducting phase. The spin polarization in the GaSb layer, which we will call *hole spin polarization*, is finite in the normal semiconducting phase if the states near the Fermi level are only electronlike. In this case the hole spin polarization does not change sign across the phase transition.

We will describe our model calculation of the subband dispersions and the wave functions in Sec. II and derive the main equations for the spin polarization in Sec. III. The numerical results are given in Sec. IV, followed by the conclusion in Sec. V.

II. SUBBAND DISPERSIONS AND WAVE FUNCTIONS

The AlSb/InAs/GaSb/AlSb system to be studied in this paper is attached at both ends to two p-doped GaSb contacts which determine the local Fermi levels. In our numerical study, the acceptor concentration is set at 10^{18} cm^{-3}. For a specific sample with a 9 nm InAs layer, 9 nm GaSb layer, and 10 nm AlSb barriers, the band edges calculated with our self-consistent scheme (to be described in the next section) are shown in Fig. 1 with a solid line for the conduction band and a dashed line for the valence band. The crystal axes are also marked in Fig. 1, and we use the z axis to specify the quantization of spin and angular momentum. A weak dc current flows along the x axis. To study the spin polarization in the quantum well of this sample, we first need to calculate the subband dispersions and the corresponding wave functions self-consistently with the potential distribution and the Fermi level position.

We generalize the model used in Ref. 28 by including the effects of strain induced by the lattice mismatch. Let us define θ as the angle between the dc current flow direction (x axis) and the in-plane wave vector $\mathbf{k}_\parallel$. Using the set of basis functions $u_1=|s_{1/2,1/2}\rangle$, $u_2=|p_{3/2,3/2}\rangle$, $u_3=|p_{3/2,-1/2}\rangle$, $u_4=|p_{1/2,-1/2}\rangle$, $u_5=|s_{1/2,-1/2}\rangle$, $u_6=|p_{3/2,-3/2}\rangle$, $u_7=|p_{3/2,1/2}\rangle$, and $u_8=|p_{1/2,1/2}\rangle$, which is given in Ref. 25, the eight-band $\mathbf{k}\cdot\mathbf{p}$ Hamiltonian for $\theta=0$ has a block-diagonal form[25]

$$\hat{H}=\begin{pmatrix}\hat{H}_+ & 0\\ 0 & \hat{H}_-\end{pmatrix}+\begin{pmatrix}\hat{H}_\epsilon & 0\\ 0 & \hat{H}_\epsilon\end{pmatrix}. \quad (1)$$

The matrices $\hat{H}_\pm$ depend on momentum operators, conduction and valence band edges, split-off energies, interband momentum matrix elements, and the modified Luttinger parameters. Their explicit forms are given in Ref. 25. The matrix $\hat{H}_\epsilon$ represents the effects of strain, and can be obtained through a unitary transformation from the strain terms in the Hamiltonian given in Ref. 27. These terms include the conduction and valence band deformation potentials, as well as the strain tensor with components ϵ_{ij}. Since our sample is grown along the y axis, $\epsilon_{xx}=\epsilon_{zz}$ and $\epsilon_{ij}=0$ for $i\neq j$. These tensor components are also similarly defined as in Ref. 27 since our quantum well structure is grown on GaSb. We should point out that we have neglected in our model Hamiltonian the linear-in-$\mathbf{k}$ terms and Kane's B-parameter, resulting from the lack of inversion symmetry in bulk zinc-blende crystals, since they are small.

Among the strain tensor components, the terms of the form $k_l\epsilon_{ij}$ can produce a significant spin split of the valence band levels in the quantum well if the GaSb layer is strained.[35] However, the heterostructures we study here are grown on GaSb, and so the GaSb layer in the quantum well is free from strain. Consequently such terms in the strain Hamiltonian have been neglected with no influence on the spin split of the hybridized electron-hole subbands and the spin polarization in our systems.

We call the two states for $\theta=0$ with opposite average spins s_z the spin-up and spin-down states, and label them by "+" and "−" respectively. Let the magnitude of $\mathbf{k}_\parallel$ be $k_\parallel\equiv|\mathbf{k}_\parallel|$. For states with $k_\parallel=k_x$, their envelope functions $\psi_+=[\psi_1\psi_2\psi_3\psi_4]^T$ and $\psi_-=[\psi_5\psi_6\psi_7\psi_8]^T$ together with the eigenenergy E satisfy the equation

$$(\hat{H}_\pm+\hat{H}_\epsilon)\psi_\pm(k_\parallel)=E\psi_\pm(k_\parallel). \quad (2)$$

The corresponding total wave functions are then $\Psi_+(\theta=0,k_\parallel)=\Sigma_{i=1}^4 u_i\psi_i$ for the spin-up states, and $\Psi_-(\theta=0,k_\parallel)=\Sigma_{i=5}^8 u_i\psi_i$ for the spin-down states. For the electronlike and the heavy-hole-like states, the so-defined spin-up (or spin-down) implies $s_z>0$ (or $s_z<0$). However, for light-hole-like states spin-up implies $s_z<0$ and spin-down $s_z>0$. The above equation will be solved together with the Poisson equation self-consistently in order to take into account the charge redistribution. The modification of the potential profile along the x axis is negligibly small because the dc current is very weak. Hence, we can write ψ_i as $\psi_i=\bar{\psi}_i(y)\exp(ik_\parallel x)$.

For hybridized electron-hole states with small in-plane wave vectors $\mathbf{k}_\parallel$ at the Fermi level, we can neglect the subband anisotropy[27] and use the scattering matrix method, which was clearly described in Refs. 25 and 28, to solve Eq. (2). The subband anisotropy in InAs/GaSb quantum wells results mainly from the strong anisotropy of the three-dimensional (3D) hole dispersions of the bulk GaSb crystal due to the difference between the second and third Luttinger parameters. Such a difference influences considerably the level positions in the InAs/GaSb quantum wells[19] and hence cannot be neglected. For the present two-dimensional (2D) case, however, the subband anisotropy is small for small $k_\parallel$ as our calculations showed. This can be explained by considering the in-plane vector $\mathbf{k}_\parallel$ as a projection of the 3D vector $\mathbf{k}_i$ of ith bulk state, which contributes to the 2D state, onto the interface plane. Roughly speaking, the 3D vector $\mathbf{k}_i$ is a sum of the $\mathbf{k}_\parallel$ and a normal "quantized" $\mathbf{k}_{i\perp}$ that depends on the well width. For a narrow well width and a small magnitude of $\mathbf{k}_\parallel$, we have $k_\parallel\ll|\mathbf{k}_{i\perp}|$ and hence the 3D vector $\mathbf{k}_i$ varies within a small angular range as $\mathbf{k}_\parallel$ rotates in a full angular range of 2π. For the small angular range of $\mathbf{k}_i$, the dispersion is approximately isotropic although the anisotropy of 3D dispersions can be significant in a large angular range.

Knowing the wave functions $\Psi_+(\theta=0,k_\parallel)$ and $\Psi_-(\theta=0,k_\parallel)$, the wave functions of the states with finite θ, $\Psi_+(\theta,k_\parallel)$ and $\Psi_-(\theta,k_\parallel)$, can be easily derived. For this purpose we replace the x-z coordinates by a new x'-z' coordinates such that the x' axis is along $\mathbf{k}_\parallel$ (namely, $x'=x\cos\theta+z\sin\theta$) and the y' axis coincides with the y axis. In the new coordinate system, we express the basis functions as

u_i'. Then the total wave functions can be expressed as $\Psi_+(\theta,k_\parallel)=\Sigma_{i=1}^4 u_i'\bar{\psi}_i(y)\exp(ik_\parallel x')$ and $\Psi_-(\theta,k_\parallel)=\Sigma_{i=5}^8 u_i'\bar{\psi}_i(y)\times\exp(ik_\parallel x')$. By writing the basis functions u_i' in terms of the functions u_i and the angle θ,[37] we obtain

$$\Psi_+(\theta,k_\parallel)=\sum_{i=1}^{8}u_i\sum_{l=1}^{4}A_{il}\psi_l\exp[ik_\parallel(x'-x)], \tag{3}$$

$$\Psi_-(\theta,k_\parallel)=\sum_{i=1}^{8}u_i\sum_{l=5}^{8}A_{il}\psi_l\exp[ik_\parallel(x'-x)], \tag{4}$$

where the matrix A is

$$A=\begin{pmatrix} c & 0 & 0 & 0 & -s & 0 & 0 & 0\\ 0 & c^3 & \sqrt{3}cs^2 & 0 & 0 & -s^3 & -\sqrt{3}c^2s & 0\\ 0 & \sqrt{3}cs^2 & c(c^2-2s^2) & 0 & 0 & -\sqrt{3}c^2s & (2c^2-s^2)s & 0\\ 0 & 0 & 0 & c & 0 & 0 & 0 & s\\ s & 0 & 0 & 0 & c & 0 & 0 & 0\\ 0 & s^3 & \sqrt{3}c^2s & 0 & 0 & c^3 & \sqrt{3}cs^2 & 0\\ 0 & \sqrt{3}c^2s & -(2c^2-s^2)s & 0 & 0 & \sqrt{3}cs^2 & c(c^2-2s^2) & 0\\ 0 & 0 & 0 & -s & 0 & 0 & 0 & c \end{pmatrix} \tag{5}$$

with $c=\cos(\theta/2)$ and $s=\sin(\theta/2)$. We should notice that when θ varies, the spin orientation of states with respect to the axis of quantization (z axis) changes. Hence, the state $\Psi_+(\pi,k_\parallel)$ [or $\Psi_-(\pi,k_\parallel)$] and the state $\Psi_+(0,k_\parallel)$ [or $\Psi_-(0,k_\parallel)$] have the same average spin but with opposite signs. To simplify the writing, we will call $\Psi_+(\theta,k_\parallel)$ the *spin-up state* and $\Psi_-(\theta,k_\parallel)$ the *spin-down state*.

III. SPIN POLARIZATION

In the absence of a dc current, the distribution function $f(E)$ of quasiparticles is reduced to its symmetric part $f_s(E)$. At temperature T it is given as

$$f_s(E)=\frac{1}{1+\exp[(E-E_F)/T]}, \tag{6}$$

where E_F is the Fermi level. Then the spin polarization in the quantum well is zero, because due to time reversal symmetry the contribution from the $s_z>0$ states with $\mathbf{k}_\parallel$ cancels that from the $s_z<0$ states with $-\mathbf{k}_\parallel$. The dc current along the x axis produces an asymmetric part of the distribution function $f_a^+(E^+,\theta,k_\parallel)$ for spin-up states, and $f_a^-(E^-,\theta,k_\parallel)$ for spin-down states. The energies $E^\pm(k_\parallel)$ of the spin-up and spin-down states are self-consistent solutions of Eq. (2) and the Poisson equation. If the level broadening $\Delta E\simeq\hbar/\tau$, where τ is the momentum relaxation time, is much less than the level separation between the spin-up and the spin-down states, we can use the Boltzmann equation to calculate $f_a^\pm(E^\pm,\theta,k_\parallel)$. Under a weak dc current, $|f_a^\pm(E^\pm,\theta,k_\parallel)|$ are much smaller than $f_s(E,\theta,k_\parallel)$. Let e be the electron charge and $v_x^\pm=\frac{1}{\hbar}\frac{dE^\pm}{dk_\parallel}\cos\theta$ the group velocities of the spin-up and spin-down states. Under a weak electric field F along the x axis, we have

$$f_a^\pm(E^\pm,\theta,k_\parallel)=|e|Fv_x^\pm\tau\frac{\partial f_s(E,\theta,k_\parallel)}{\partial E}. \tag{7}$$

To calculate the density of spin polarization in the InAs/GaSb quantum well, we assume that in the xz plane the sample is bounded spatially in the area $0\leqslant x\leqslant 1$ and $0\leqslant z\leqslant 1$. Along the y axis, the InAs layer is in the region $0=y_1^e\leqslant y\leqslant y_2^e$ and the GaSb in the region $y_2^e=y_1^h\leqslant y\leqslant y_2^h$. In terms of the Pauli spin matrix σ_z, the average values of electron spins $\langle s_e^\pm\rangle$ for the spin-up and the spin-down states are calculated as

$$\langle s_e^\pm\rangle=\int_{y_1^e}^{y_2^e}dy\int_0^1dx\int_0^1dz\ \Psi_\pm^\dagger(\theta,k_\parallel)\frac{1}{2}\sigma_z\Psi_\pm(\theta,k_\parallel). \tag{8}$$

Similarly, the average values of hole spins $\langle s_h^\pm\rangle$ for the spin-up and the spin-down states are

$$\langle s_h^\pm\rangle=\int_{y_1^h}^{y_2^h}dy\int_0^1dx\int_0^1dz\ \Psi_\pm^\dagger(\theta,k_\parallel)\frac{1}{2}\sigma_z\Psi_\pm(\theta,k_\parallel). \tag{9}$$

In terms of $\langle s_e^\pm\rangle$ and $\langle s_h^\pm\rangle$, the densities of spin polarization of electrons S_e in the InAs layer and of holes S_h in the GaSb layer are then readily obtained as

$$S_{e,h}=\frac{1}{(2\pi)^2}\int[f_a^+(E^+,\theta,k_\parallel)\langle s_{e,h}^+\rangle+f_a^-(E^-,\theta,k_\parallel)\langle s_{e,h}^-\rangle]k_\parallel dk_\parallel d\theta. \tag{10}$$

If several subbands contribute to the spin polarization, then a summation should also be taken over all these subbands at the right side of Eq. (10).

We define $\phi_\pm(\theta,k_\parallel)$ as the eight-component envelope functions corresponding to the total wave functions

$\Psi_{\pm}(\theta,k_{\parallel})$. Then Eqs. (8) and (9) can be rewritten as

$$\langle s_e^{\pm}\rangle = \int_{y_1^e}^{y_2^e} dy\ \phi_{\pm}^{\dagger}(\theta,k_{\parallel}) B \phi_{\pm}(\theta,k_{\parallel}), \tag{11}$$

$$\langle s_h^{\pm}\rangle = \int_{y_1^h}^{y_2^h} dy\ \phi_{\pm}^{\dagger}(\theta,k_{\parallel}) B \phi_{\pm}(\theta,k_{\parallel}). \tag{12}$$

In the above equations, the 8×8 matrix B has a block-diagonal form

$$B = \frac{1}{2}\begin{pmatrix} B_+ & 0 \\ 0 & B_- \end{pmatrix}, \tag{13}$$

where the 4×4 matrices $B_{\pm}$ are given by

$$B_{\pm} = \begin{pmatrix} \pm 1 & 0 & 0 & 0 \\ 0 & \pm 1 & 0 & 0 \\ 0 & 0 & \mp 1/3 & \pm 2\sqrt{2}/3 \\ 0 & 0 & \pm 2\sqrt{2}/3 & \pm 1/3 \end{pmatrix}. \tag{14}$$

Substituting $\langle s_{e,h}^{\pm}\rangle$ from Eqs. (11) and (12), and $f_a^{\pm}(E^{\pm},\theta,k_{\parallel})$ from Eq. (7) into Eq. (10), using Eqs. (3)–(5) and integrating over the angle θ in Eq. (10), we obtain a compact expression for $S_{e,h}$ as

$$S_{e,h} = \frac{|e|F\tau}{8\pi\hbar}\int\left(\frac{dE^+}{dk_{\parallel}}\frac{\partial f_s}{\partial E}G_{e,h}^{+} - \frac{dE^-}{dk_{\parallel}}\frac{\partial f_s}{\partial E}G_{e,h}^{-}\right)k_{\parallel}dk_{\parallel}, \tag{15}$$

where

$$G_{e,h}^{+} = \int_{y_1^{e,h}}^{y_2^{e,h}} (|\psi_1|^2 + |\psi_2|^2 - |\psi_3|^2/3 + |\psi_4|^2/3)dy, \tag{16}$$

and

$$G_{e,h}^{-} = \int_{y_1^{e,h}}^{y_2^{e,h}} (|\psi_5|^2 + |\psi_6|^2 - |\psi_7|^2/3 + |\psi_8|^2/3)dy. \tag{17}$$

We would like to remind the reader that the envelope functions ψ_i in Eqs. (16) and (17) are the components of $\psi_+(k_{\parallel})$ and $\psi_-(k_{\parallel})$, respectively, which are solutions of Eq. (2) for $\theta=0$.

We should point out that the growth direction of our sample is the y axis and that a weak electric field is applied along the x axis. The z axis is chosen to be the quantization axis of spin and angular momentum. In this case, similar model calculations do not indicate any spin polarization of electrons or holes along the x and y axes.

IV. RESULTS AND DISCUSSION

To perform numerical calculations we set the temperature at 1.5 K, the relaxation time $\tau=10^{-11}$ seconds, and the applied parallel dc electric field 25 V/cm. The material parameters and the band offsets are taken from Refs. 23 and 27.

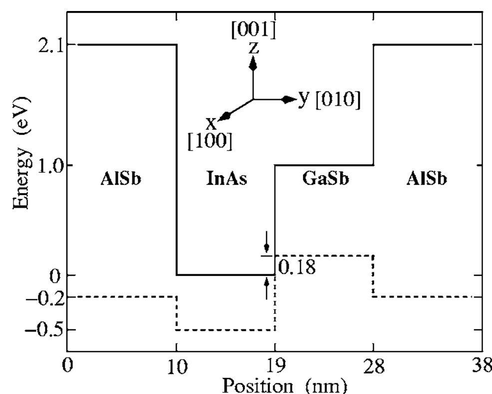

FIG. 1. The self-consistent energy band diagram of the AlSb/InAs/GaSb/AlSb quantum well with a 9 nm InAs layer and a 9 nm GaSb layer. The solid curves are for the conduction band edge and the dashed curves are for the valence band edge.

Since the dispersions of AlSb/InAs/GaSb/AlSb quantum wells are dominated by the InAs layer width W_e and the GaSb layer width W_h, these two are the varying parameters in our numerical study. The sample shown in Fig. 1 has W_e=9 nm and W_h=9 nm. We should mention that the asymmetric parts of the distribution functions $f_a^{\pm}(E^{\pm},\theta,k_{\parallel})$ are significant only near the Fermi level, and the spin polarization of the system is mainly contributed by the subbands around this energy region. Consequently, in our numerical results we will present only the lowest electronlike subband $1e$ and the highest heavy-hole-like subband $1hh$ in the quantum well. These subbands are labeled according to the wave-function properties of the corresponding states at zone center $k_{\parallel}=0$.

The calculated dispersions are shown in Fig. 2(a) for $(W_e,W_h)=(9,3)$ nm, and Fig. 2(b) for $(W_e,W_h)=(9,9)$ nm. The solid curves are for the spin-up states and the dashed curves are for the spin-down states. The electron-hole system

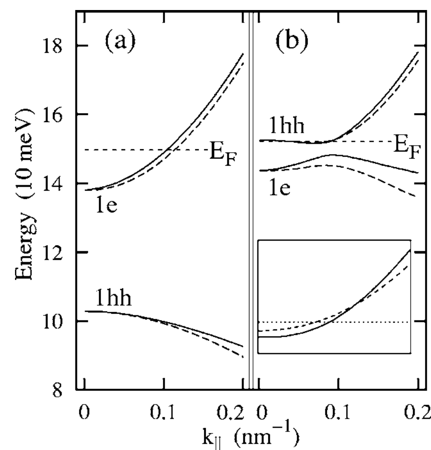

FIG. 2. The $1e$ and $1hh$ subband dispersions in the InAs/GaSb quantum well with a 9 nm InAs layer. The GaSb layer thickness is 3 nm for panel (a) and 9 nm for panel (b). Inset in panel (b) is a magnification of a neighborhood of the location where the Fermi level crosses the electronlike levels. The zero energy is set at the InAs conduction band edge at the AlSb/InAs interface. Solid curves are for the spin-up states and dashed curves the spin-down states.

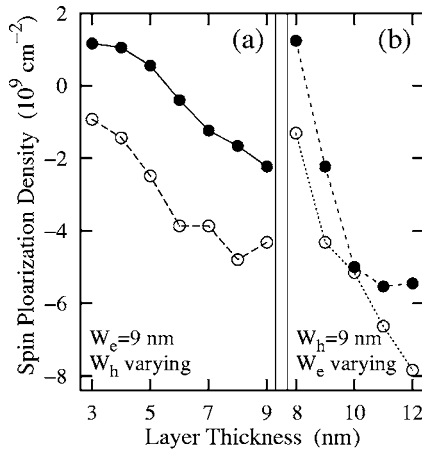

FIG. 3. Spin polarization density of electrons in the InAs layer (solid dots) and of holes in the GaSb layer (open circles) as functions of the layer thickness. For panel (a) the InAs layer is 9 nm but with varying GaSb layer width, and for panel (b) the GaSb layer is 9 nm but with varying InAs layer width.

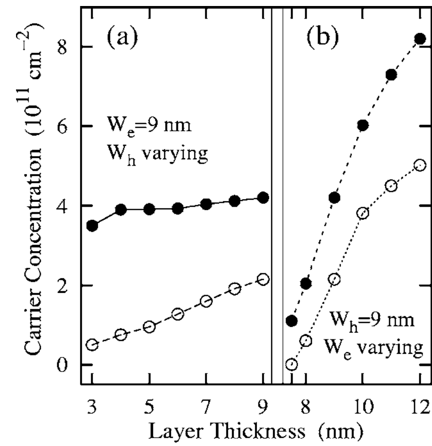

FIG. 4. Electron concentration in the InAs layer (solid dots) and hole concentration in the GaSb layer (open circles) as functions of the layer thickness. For panel (a) the InAs layer is 9 nm but with varying GaSb layer width, and for panel (b) the GaSb layer is 9 nm but with varying InAs layer width.

corresponding to Fig. 2(a) is in a normal semiconducting (NSC) phase because the lowest electron level is higher than all hole levels. With increasing GaSb layer thickness W_h, the $1hh$ level at $k_\parallel=0$ moves upwards, and eventually lies above the $1e$ as shown in Fig. 2(b) for $W_h=9$ nm. As the in-plane wave vector $k_\parallel$ increases, the electronlike states and the heavy-hole-like states approach each other and anticross, resulting in a hybridization gap in the in-plane dispersions. After the anticrossing, the $1hh$ subband becomes electronlike while the $1e$ subband becomes heavy-hole-like. Such a system is in a hybridized semiconducting (HSC) phase. The Fermi level E_F crosses only the $1e$ subband in Fig. 2(a), and only the $1hh$ subband in Fig. 2(b) as shown by the inset. Hence, the main contribution to the spin polarization is from the $1e$ subband for the sample with $W_h=3$ nm, but from the $1hh$ subband for the sample with $W_h=9$ nm.

To investigate in details the effect of InAs and GaSb layer widths, we have calculated the spin-polarization density with fixed $W_e=9$ nm (or $W_h=9$ nm) but varying W_h (or W_e). The results are shown in Fig. 3 with solid dots for the electron spin polarization in the InAs layer and open circles for the hole spin polarization in the GaSb layer. Figure 3(a) is for constant $W_e=9$ nm and Fig. 3(b) is for constant $W_h=9$ nm. It is important to notice in Fig. 3(a) a finite value of hole spin polarization even in the NSC for $W_h=3$ nm, where almost all holelike states are occupied by electrons. The origin of this hole spin polarization is the hybridization of the electronlike states with the light-hole states.[23] Around $W_h \simeq 5.5$ nm where the system transforms from the NSC phase to the HSC phase, the electron spin polarization changes sign from positive to negative. This is because the spin-splitting of the electronlike levels near the Fermi energy changes sign, as indicated in Fig. 2(b). On the other hand, the hole spin polarization remains negative in both the NSC and HSC phases. For the two phases in Fig. 3(a) with $W_h=3$ nm and $W_h=9$ nm, the signs of the total spin polarization are also different.

For a fixed GaSb layer thickness at $W_h=9$ nm, the NSC to HSC phase transition occurs when the InAs layer width W_e increases to about 8.5 nm. When W_e is reduced to 7.5 nm, the Fermi level moves into the semiconducting gap, and so the total spin polarization of the entire system vanishes. As shown in Fig. 3(b), when W_e increases across the NSC-HSC phase boundary, the electron spin polarization changes sign but not the hole spin polarization. We found several interesting phenomena. Because of its larger spin split, the hybridized electronlike states give the main contribution to the spin polarization in both the InAs and GaSb layers. Also, in the HSC phase, because the electron spin polarization of the spin-up states almost compensates that of the spin-down states, the electron spin polarization is less than the hole spin polarization. Finally, the hybridization of electrons and holes for spin-up states differs significantly from that for spin-down states, resulting in a strong spin polarization in the GaSb layer.

Similar to the plots in Fig. 3 for the spin-polarization density, plots of carrier concentration are shown in Fig. 4 with solid dots for the electron concentration n in the InAs layer and open circles for the hole concentration p in the GaSb layer. In all samples specified in this figure, n is larger than p. Due to hybridization of the empty electronlike states with the light-hole states,[23,25] there exists a small finite hole concentration in the NSC phase. With increasing GaSb layer width W_h in Fig. 4(a), the $1hh$ level at $k_\parallel=0$ moves to above the Fermi energy. Hence, p increases with W_h but n remains almost unchanged. On the other hand, with increasing InAs layer width W_e in Fig. 4(b), n increases rapidly because the $1e$ level moves to lower energy. Such process of lowering the $1e$ level also increases p for the reason that electrons can flow into the InAs layer not only from the GaSb contacts but also from the GaSb valence band in the quantum well.

With increasing both the InAs layer thickness and the GaSb layer thickness, the semimetallic phase can be realized. Then there is no forbidden energy interval in the in-plane dispersion. The semimetallic phase can be achieved at zero bias for the quantum well with a 15 nm InAs layer and a 10 nm GaSb layer as our calculations showed. In this case

the hybridization gaps for the spin-up and spin-down states do not overlap. Also, with increasing in-plane wave vector, the spin split of $1hh$ subband states, which contribute to most of the spin polarization, changes sign twice. As a result, our model gives a positive spin polarization of electrons in the InAs layer and a negative spin polarization of holes in the GaSb layer for this structure. However, when the layer gets thicker, the in-plane wave vector $\mathbf{k}_{\parallel}$ of electronlike states at the Fermi level gets larger and its magnitude can become comparable to the magnitudes of the 3D wave vectors of hole bulk states in the GaSb layer, which contribute to the 2D electronlike states. Hence, to derive accurate results of spin polarization, the anisotropy of subband dispersions should be been taken into account in our calculations.

Let us define the fraction of spin-polarized carriers $\nu_e = |S_e|/ns_z^e$ for electrons, and $\nu_h = |S_h|/ps_z^h$ for holes, where $s_z^{e,h} = \frac{1}{2}$. From Figs. 3 and 4, we see that for the parameters used in our calculation, both ν_e and ν_h are of the order of 1%. However, Eq. (15) indicates that the fraction of spin-polarized carriers can be easily enhanced by applying a stronger dc electric field. On the other hand, when the electric field becomes sufficiently large, the drift velocities of the hybridized electron-hole states become of the same order as the corresponding group velocities. The approximation of small asymmetry of the distribution function is no longer valid and the scattering processes between the spin-up and spin-down states will decrease the spin polarization. Hence, the 100% spin polarization cannot be achieved by increasing the dc electric field. We believe that the maximum value of spin polarization, which can be achieved in the broken-gap quantum wells, is greater than that in type I asymmetric heterostructures, because the spin-dependent hybridization of electron and hole states can significantly enhance the spin polarization.

Let us discuss the validity of the approximations used in our study of the quasiparticle spin polarization. First, corresponding to the momentum relaxation time $\tau = 10^{-11}$ s, the electron mobility is about 10^5 cm^2/(Vs) and the hole mobility about 10^4 cm^2/(Vs). Then, at a field strength $F \simeq 25$ V/cm, the drift velocity is about 10^6 cm/s for electrons and 10^5 cm/s for holes. Since these drift velocities are much less than the corresponding group velocities at the Fermi energy, our approximation of small asymmetry of the distribution function is valid.

We have neglected the bulk asymmetry terms which are proportional to Kane's B parameter. It was shown in Ref. 8 that if the in-plane wave vectors are larger than 0.3 nm^{-1}, the effect of these terms on the spin split of electron levels cannot be ignored. However, for the quantum wells studied here, the Fermi wave vector is about 0.1 nm^{-1}. Consequently, the spin split due to these bulk asymmetry terms is at least one order of magnitude less than that produced by the Rashba effect for all states which contribute to the spin polarization.

Finally, for $\tau = 10^{-11}$ s, the corresponding level broadening is less than 0.1 meV. Therefore we can use the Boltzmann equation to calculate spin polarization. However, in low quality samples with higher defect concentration, the carrier mobility can be suppressed.[38] In this situation the level broadening is large and so quantum kinetic theory should be used to study the spin polarization.

To close this section, we will outline two possible experimental detections of spin polarization in the InAs/GaSb quantum wells. The first one involves the investigation of the frequency shift of nuclear magnetic resonance (NMR) in our samples. Such a method was proposed in Ref. 3 to detect the electron spin polarization in type I quantum wells with a lateral current. Since the wave function of the conduction band electron has a large component of s-type functions, it has a finite value at the location of each constitutive atom. Hence, there is a contact interaction between an electron spin and spins of Ga and In nuclei in the heterostructure. The corresponding shift in NMR frequency can be observed experimentally, if the concentration of spin-polarized electrons is sufficiently high. The spins of holes, whose wave functions have large components of p-type functions, can also interact with the nuclear spins through the dipole-dipole interaction. Also, the holes in our structures are hybridized with the electrons. Hence, the contact interaction between the spins of holelike states and nuclei is finite.

The second approach, which is sensitive even for weak spin polarization of carriers in the quantum wells, is the optical method. It was proposed in Ref. 5 that the electron spin polarization in type-I quantum wells can be detected by measuring the polarization of photons emitted during the electron-hole recombination. The probability of the emitted light being right-handed or left-handed circular polarized depends on the occupation probability of various electron spin states. Similarly, in the quantum wells with spin-split subbands, the interband or intersubband absorption of circular polarized light by carriers also depends on the occupation probability of their spin states.[39] Then, for a quantum well with spin-polarized carriers, its absorption coefficient for the right-handed circular polarized light is different from that for the left-handed circular polarized light. Such a difference can be observed experimentally. It is important to notice that the spin polarization of quasiparticles near the Fermi level is much stronger than the average spin polarization. Hence, by a proper tuning of the light frequency to select the optical transitions from the states near the Fermi level, the detected carrier spin polarization can be enhanced.

V. CONCLUSION

We have developed a theory of the spin polarization of quasiparticles in nonmagnetic asymmetric quantum wells under a dc current parallel to interfaces. We have used the eight-band $\mathbf{k} \cdot \mathbf{p}$ model including coupling of electron states, light-hole states, heavy-hole states, and the states in the split-off band. The spin split of subbands due to the spin-orbit interaction and the structure asymmetry, together with the existence of nonequilibrium distribution function of carriers, have generated interesting phenomena which are studied in details. Assuming a small asymmetry of the distribution functions our theory is based on solving the Boltzmann equation for the hybridized electron-hole states. To present accurate numerical results, we have analyzed the spin polarizations of electrons and holes in InAs/GaSb quantum wells. We have demonstrated the important effect of electron-hole

hybridization on the spin polarizations in both the InAs layer and the GaSb layer. For a very weak asymmetry of the distribution function, the spin polarization of both electrons and holes can reach about 1%.

ACKNOWLEDGMENT

This work was financially supported by the RFBR (Grant No. 03-02-16788).

[1] *Semiconductor Spintronics and Quantum Computation*, edited by D. D. Awschalom, D. Loss, and N. Samarth (Springer-Verlag, Berlin, 2002); G. Schmidt, J. Phys. D **38**, R107 (2005).
[2] F. T. Vasko and N. A. Prima, Sov. Phys. Solid State **21**, 994 (1979).
[3] V. M. Edelstein, Solid State Commun. **73**, 233 (1990).
[4] A. G. Aronov, Yu. B. Lyanda-Geller, and G. E. Pikus, Zh. Eksp. Teor. Fiz. **100**, 973 (1991).
[5] A. G. Mal'shukov and K. A. Chao, Phys. Rev. B **65**, 241308 (2002).
[6] Jun-ichiro Inoue, Gerrit E. W. Bauer, and Laurens W. Molenkamp, Phys. Rev. B **67**, 033104 (2003).
[7] E. G. Mishchenko, A. V. Shytov, and B. I. Halperin, Phys. Rev. Lett. **93**, 226602 (2004).
[8] I. Vurgaftman and J. R. Meyer, Phys. Rev. B **70**, 115320 (2004).
[9] R. Winkler, Phys. Rev. B **70**, 125301 (2004).
[10] R. Winkler, Phys. Rev. B **71**, 113307 (2005).
[11] A. Zakharova, F. T. Vasko, and V. Ryzhii, J. Phys.: Condens. Matter **6**, 7537 (1994).
[12] A. Voskoboynikov, S. S. Liu, C. P. Lee, and O. Tretyak, J. Appl. Phys. **87**, 387 (2000).
[13] M. Kohda, Y. Ohno, Y. Takamura, F. Matsukora, and H. Ohno, Jpn. J. Appl. Phys., Part 2 **40**, L1274 (2001).
[14] David Z.-Y. Ting and X. Cartoixa, Phys. Rev. B **68**, 235320 (2003).
[15] I. Vurgaftman and J. R. Meyer, Phys. Rev. B **67**, 125209 (2003).
[16] A. G. Petukhov, D. O. Demchenko, and A. N. Chantis, Phys. Rev. B **68**, 125332 (2003).
[17] M. M. Glazov, P. S. Alekseev, M. A. Odnoblyudov, V. M. Chistyakov, S. A. Tarasenko, and I. N. Yassievich, Phys. Rev. B **71**, 155313 (2005).
[18] P. Krstajic and F. M. Peeters, Phys. Rev. B **71**, 115321 (2005).
[19] A. Zakharova, K. Nilsson, K. A. Chao, and S. T. Yen, Phys. Rev. B **72**, 115329 (2005).
[20] M. Altarelli, Phys. Rev. B **28**, 842 (1983).
[21] Y. Naveh and B. Laikhtman, Appl. Phys. Lett. **66**, 1980 (1995).
[22] A. J. L. Poulter, M. Lakrimi, R. J. Nicholas, N. J. Mason, and P. J. Walker, Phys. Rev. B **60**, 1884 (1999).
[23] E. Halvorsen, Y. Galperin, and K. A. Chao, Phys. Rev. B **61**, 16743 (2000).
[24] R. Magri, L. W. Wang, A. Zunger, I. Vurgaftman, and J. R. Meyer, Phys. Rev. B **61**, 10235 (2000).
[25] A. Zakharova, S. T. Yen, and K. A. Chao, Phys. Rev. B **64**, 235332 (2001).
[26] R. Magri and A. Zunger, Phys. Rev. B **65**, 165302 (2002).
[27] A. Zakharova, S. T. Yen, and K. A. Chao, Phys. Rev. B **66**, 085312 (2002).
[28] I. Lapushkin, A. Zakharova, S. T. Yen, and K. A. Chao, J. Phys.: Condens. Matter **16**, 4677 (2004).
[29] M. Lakrimi, S. Khym, R. J. Nicholas, D. M. Symons, F. M. Peeters, N. J. Mason, and P. J. Walker, Phys. Rev. Lett. **79**, 3034 (1997).
[30] M. J. Yang, C. H. Yang, B. R. Bennett, and B. V. Shanabrook, Phys. Rev. Lett. **78**, 4613 (1997).
[31] L. J. Cooper, N. K. Patel, V. Drouot, E. H. Linfield, D. A. Ritchie, and M. Pepper, Phys. Rev. B **57**, 11915 (1998).
[32] M. J. Yang, C. H. Yang, and B. R. Bennett, Phys. Rev. B **60**, R13958 (1999).
[33] E. I. Rashba, Sov. Phys. Solid State **2**, 1109 (1960); Yu. A. Bychkov and E. I. Rashba, JETP Lett. **39**, 78 (1984).
[34] X. Cartoixa, D. Z.-Y. Ting, and T. C. McGill, Phys. Rev. B **68**, 235319 (2003).
[35] O. Mauritz, and U. Ekenberg, Phys. Rev. B **55**, 10729 (1997).
[36] J. Luo, H. Munekata, F. F. Fang, and P. J. Stiles, Phys. Rev. B **38**, R10142 (1988); **41**, 7685 (1990).
[37] E. L. Ivchenko and G. E. Pikus, *Superlattices and Other Hetrostructures* (Springer, Berlin, 1997).
[38] K. Suzuki, S. Miyashita, and Y. Hirayama, Phys. Rev. B **67**, 195319 (2003).
[39] S. D. Ganichev and W. Prettl, J. Phys.: Condens. Matter **15**, R935 (2003).